MATEC Web of Conferences **83**, 02003 (2016) DOI: 10.1051/matecconf/20168302003
CSNDD 2016

Homotopy analysis approach for nonlinear piezoelectric vibration energy harvesting

Shahram Shahlaei-Far[1,*], Airton Nabarrete[1], and José Manoel Balthazar[1]

[1]Instituto Tecnológico de Aeronáutica - ITA, Enghenaria Aeronáutica e Mecânica, 12208-900, São José dos Campos, Brazil

Abstract. Piezoelectric energy harvesting from a vertical geometrically nonlinear cantilever beam with a tip mass subject to transverse harmonic base excitations is analyzed. One piezoelectric patch is placed on the slender beam to convert the tension and compression into electrical voltage. Applying the homotopy analysis method to the coupled electromechanical governing equations, we derive analytical solutions for the horizontal displacement of the tip mass and consequently the output voltage from the piezoelectric patch. Analytical approximation for the frequency response and phase of the geometrically forced nonlinear vibration system are also obtained. The research aims at a rigorous analytical perspective on a nonlinear problem which has previously been solely investigated by numerical and experimental methods.

1 Introduction

Piezoelectric transduction for vibration-based energy harvesting plays an important role for remote/wireless sensor systems. This vibration-to-electric energy conversion mechanism uses the ambient vibration energy to power and/or to recharge such electronic components. Usually, as in the case of resonance-based energy harvesting, the piezoelectric effect is achieved by fixing a cantilever beam with one or two piezoceramic layers on a host structure and using single excitation frequency. The piezoelectric effect converts mechanical strain induced in the layers into an electric current generating alternating voltage [1,2].

Requiring an energy harvester to harvest a reasonable amount of energy when the excitation frequency is low can be a difficult undertaking as the physical dimensions of the devices are small. Maximizing the harvested energy over a wide range of excitation frequencies is achieved by implementing nonlinear structural systems and using a double potential well function [3].

In this study, an inverted cantilever beam with piezoelastic patch and a tip mass is mounted vertically on an energy harvesting device and is subjected to transverse base excitations. [4]

Applying the homotopy analysis method (HAM), introduced by Shijun Liao [5], to the coupled electromechanical governing equations of motion, novel analytical solutions of the horizontal displacement coordinate, of its amplitude and phase as well as the output voltage are derived. The aim is to address the subject of piezoelectric energy harvesting from a purely analytical perspective emphasizing the capabilities of a first-order approximation of HAM to present highly accurate closed-form solutions.

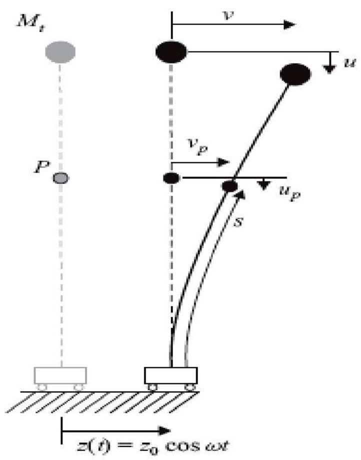

Fig. 1. Inverted cantilever beam with tip mass on host structure subject to transverse excitation [4]

2 Governing equations

The coupled electromechanical governing equations for the beam-mass system are [4]

$$[N_5^2 I_t + M_t + \rho\bar{A}N_1 + (\rho\bar{A}N_3 + M_t N_4^2 + N_5^4 I_t)v^2] + (\rho\bar{A}N_3 + M_t N_4^2 + N_5^4 I_t)v\dot{v}^2 + \theta_1 V - \theta_2 v^2 V = -(\rho\bar{A}N_2 + M_t)\ddot{z} \quad (1)$$

and

$$C_p\dot{V} + \frac{V}{R_l} + \theta_1\dot{v} + \theta_2 v^2\dot{v} = 0 \quad (2)$$

*Corresponding author: shazzz_85@yahoo.de

subject to

$$v(0) = A, \dot{v}(0) = 0 \text{ and } V(0) = 0 \quad (3)$$

where v is the horizontal elastic displacement at the tip mass, V is the voltage output of the piezoelectric patch, L is the length of the beam, $\bar{A}$ is its cross-sectional area, ρ is the mass density, E is the equivalent Young's modulus, I is the second moment of area, M_t is the tip mass of the beam, I_t is its moment of inertia, θ_1 and θ_2 are parameters for work done by the piezoelectric patch, C_p is its capacitance, R_l is the load resistor and g is the gravitational constant. The values of the parameters N_i, $i = 1,2,\ldots,6$, θ_1 and θ_2 are given in Table 1.

For our analysis, we consider the time domain between $t = 1300s$ and $t = 1500s$ to demonstrate nonlinear dynamical characteristics of the steady state region. First, we solve Eq. (2) to obtain a solution for V as a function of v and $\dot{v}$ considering when the tip mass oscillates close to one of the equilibrium positions. The amplitude of oscillation of the horizontal displacement is very small (the velocity being even considerably smaller), thus the expression containing v and $\dot{v}$ in (2) can be approximated by a constant value. Substituting the obtained solution expression of V into Eq. (1) we gain a single differential equation dependent on v. Finally, we substitute the solution of v into the expression for V. Solving Eq. (2) we obtain

$$V(\dot{v}, v, t) = KC_pR_l\left(1 - e^{-\frac{1}{C_pR_l}t}\right) \quad (4)$$

where

$$K = -\frac{\theta_1\dot{v} + \theta_2 v^2\dot{v}}{C_p} \quad (5)$$

For large values of t as considered here, the term $e^{-\frac{1}{C_pR_l}t}$ becomes negligible (see values for C_p and R_l), thus, in our case, Eq. (4) is simplified and reduced to

$$V(\dot{v}, v, t) = -R_l\dot{v}(\theta_1 + \theta_2 v^2) \quad (6)$$

Inserting Eq. (6) into Eq. (1) we have

$$\begin{aligned} &C_1\ddot{v} + C_2v^2\ddot{v} + C_3v\dot{v}^2 + C_4v + C_5v^3 + \\ &\theta_1^2R_l\dot{v} + 2\theta_1\theta_2R_l\dot{v}v^2 + \theta_2^2R_l\dot{v}v^4 \\ &= C_6z_0\Omega^2\cos(\Omega t - \varphi) \end{aligned} \quad (7)$$

where the constants C_i, $i = 1,2,..,6$ are given in Table 1. Note that, without loss of generality, we can introduce the phase angle φ in the expression of the harmonic load as a quantity to be determined. The solution derivation uses the approach described in [6] for nonlinear problems of forced vibrations.

Defining the variables

$$\tau = \Omega t, v(t) = Au(\tau) \quad (8)$$

and inserting them into Eq. (7), we obtain

$$\begin{aligned} &C_1A\Omega^2\frac{\partial^2u(\tau)}{\partial\tau^2} + C_2A^3\Omega^2\frac{\partial^2u(\tau)}{\partial\tau^2}u^2 + \\ &C_3A^3\Omega^2u\left(\frac{\partial u(\tau)}{\partial\tau}\right)^2 + C_4Au + C_5A^3u^3 + \\ &\theta_1^2R_lA\Omega\frac{\partial u(\tau)}{\partial\tau} + +2\theta_1\theta_2R_lA^3\Omega\frac{\partial u(\tau)}{\partial\tau}u^2 + \\ &\theta_2^2R_lA^5\Omega\frac{\partial u(\tau)}{\partial\tau}u^4 = \mathrm{F}_1\cos(\tau) + \mathrm{F}_2\sin(\tau) \end{aligned} \quad (9)$$

subject to the initial conditions

$$u(0) = 1, \frac{\partial u(0)}{\partial\tau} = 0 \quad (10)$$

with the constants F_1 and F_2 satisfying

$$(F_1^2 + F_2^2)^{\frac{1}{2}} = C_6z_0\Omega^2, \varphi = \tan^{-1}\left(\frac{F_2}{F_1}\right) \quad (11)$$

3 Homotopy analysis method

The periodic solution to Eq. (9) can be expressed by a set of base functions

$$\{\sin(m\tau), \cos(m\tau) \mid m = 1,2,3,\ldots\} \quad (12)$$

such that

$$u(\tau) = \sum_{k=1}^{\infty}(\alpha_k\sin(k\tau) + \beta_k\cos(k\tau)) \quad (13)$$

where α_k and β_k are coefficients to be determined. We choose the initial guess as

$$u_0(\tau) = \cos(\tau) \quad (14)$$

which satisfies the initial conditions of Eq. (10). We choose the linear operator to be

$$\boldsymbol{\mathcal{L}}[\phi(\tau, q)] = \Omega^2\left(\frac{\partial^2\phi(\tau, q)}{\partial\tau^2} + \phi(\tau, q)\right) \quad (15)$$

with the property

$$\boldsymbol{\mathcal{L}}[D_1\sin(\tau) + D_2\cos(\tau)] = 0 \quad (16)$$

where D_1 and D_2 are constants of integration. According to Eq. (9), we define the nonlinear operator

$$\begin{aligned} &\boldsymbol{\mathcal{N}}[\phi(\tau, q), \Lambda(q)] = C_1\Lambda(q)\Omega^2\frac{\partial^2\phi(\tau, q)}{\partial\tau^2} + \\ &C_2\Lambda(q)^3\Omega^2\frac{\partial^2\phi(\tau, q)}{\partial\tau^2}\phi(\tau, q)^2 + \\ &C_3\Lambda(q)^3\Omega^2\phi(\tau, q)\left(\frac{\partial\phi(\tau, q)}{\partial\tau}\right)^2 + C_4\Lambda(q)\phi(\tau, q) + \\ &C_5\Lambda(q)^3\phi(\tau, q)^3 + \theta_1^2R_l\Lambda(q)\Omega\frac{\partial\phi(\tau, q)}{\partial\tau} \\ &+2\theta_1\theta_2R_l\Lambda(q)^3\Omega\frac{\partial\phi(\tau, q)}{\partial\tau}\phi(\tau, q)q)^2 + \\ &\theta_1^2R_l\Lambda(q)^5\Omega\frac{\partial\phi(\tau, q)}{\partial\tau}\phi(\tau, q)^4 - \mathrm{F}_1\cos(\tau) - \\ &\mathrm{F}_2\sin(\tau) \end{aligned} \quad (17)$$

where $q \in [0,1]$ is an embedding parameter, $\phi(\tau, q)$ is a function of τ and q, $\Lambda(q)$ is a function of q. The zero-order deformation equation is given by

$$\begin{aligned} &(1 - q)\boldsymbol{\mathcal{L}}[\phi(\tau, q) - u_0(\tau)] \\ &= qc_0H(\tau)\boldsymbol{\mathcal{N}}[\phi(\tau, q), \Lambda(q)] \end{aligned} \quad (18)$$

where $c_0 \neq 0$ is the convergence-control parameter and $H(\tau)$ a nonzero auxiliary function. For $q = 0$ and $q = 1$ we have

$$\phi(\tau, 0) = u_0(\tau), \phi(\tau, 1) = u(\tau) \tag{19}$$

$$\Lambda(0) = A_0, \Lambda(1) = A \tag{20}$$

Thus, the function $\phi(\tau, q)$ varies from the initial guess $u_0(\tau)$ to the desired solution as q varies from 0 to 1. The Taylor expansions of $\phi(\tau, q)$ and $\Lambda(q)$ with respect to q are

$$\phi(\tau, q) = u_0(\tau) + \sum_{m=1}^{\infty} u_m(\tau)\, q^m \tag{21}$$

$$\Lambda(q) = A_0 + \sum_{m=1}^{\infty} A_m\, q^m \tag{22}$$

where

$$u_m(\tau) = \frac{1}{m!} \frac{\partial^m \phi(\tau, q)}{\partial q^m} |_{q=0} \tag{23}$$

$$A_m = \frac{1}{m!} \frac{\partial^m \Lambda(q)}{\partial q^m} |_{q=0} \tag{24}$$

Choosing properly the auxiliary function $H(\tau)$ and the convergence-control parameter c_0, the series in Eqs. (23) and (24) converge when $q = 1$, such that

$$u(\tau) = u_0(\tau) + \sum_{m=1}^{\infty} u_m(\tau) \tag{25}$$

$$A = A_0 + \sum_{m=1}^{\infty} A_m \tag{26}$$

Differentiating the zero-order equation (18) m times with respect to q, dividing it by $m!$ and setting $q = 0$, the m^{th}-order deformation equation is obtained as

$$\boldsymbol{\mathcal{L}}[u_m(\tau) - \chi_m u_{m-1}(\tau)] = c_0 H(\tau) R_{\boldsymbol{m}}(\vec{u}_{m-1}, \vec{A}_{m-1}) \tag{27}$$

subject to the initial conditions

$$u_m(0) = \frac{\partial u_m(0)}{\partial \tau} = 0 \tag{28}$$

where

$$\chi_m = \begin{cases} 0 & m \leq 1 \\ 1 & m > 1 \end{cases} \tag{29}$$

$$\vec{u}_{m-1} = \{u_0(\tau), u_1(\tau), \ldots, u_{m-1}(\tau)\}, \quad \vec{A}_{m-1} = \{A_0, A_1, \ldots, A_{m-1}\} \tag{30}$$

$$R_{\boldsymbol{m}}(\vec{u}_{m-1}, \vec{A}_{m-1}) = \frac{1}{(m-1)!} \frac{d^{m-1} \boldsymbol{\mathcal{N}}[\phi(\tau, q), \Lambda(q)]}{d q^{m-1}} |_{q=0} \tag{31}$$

For the nonzero auxiliary function to obey the *rule of solution expression* and the *rule of coefficient ergodicity*, we choose it to be

$$H(\tau) = \cos(2\kappa\tau) \tag{32}$$

where κ is an integer. It can be determined uniquely as $H(\tau) = 1$.

The general solution to Eq. (26) for $m \geq 1$ is derived to be

$$u_m(\tau) = D_1 \sin(\tau) + D_2 \cos(\tau) + \chi_m u_{m-1}(\tau) + \frac{c_0}{\Omega^2} \sum_{k=1}^{l(m)} \frac{(c_{m,k} \cos((2k+1)\tau) + d_{m,k} \sin((2k+1)\tau))}{1-(2k+1)^2} \tag{33}$$

where D_1 and D_2 need to be determined by the initial conditions in Eq. (28).

For a first-order homotopy approximation ($m = 1$), we obtain from Eq. (31) the right-hand side of the first-order deformation equation (27) as

$$R_{\boldsymbol{1}}(\vec{u}_0, \vec{A}_0) = \left(-C_1 A_0 \Omega^2 - \frac{3}{4} C_2 A_0^3 \Omega^2 + \frac{1}{4} C_3 A_0^3 \Omega^2 + C_4 A_0 + \frac{3}{4} C_5 A_0^3 - F_1\right) \cos(\tau) + \left(-\theta_1^2 R_l A_0 \Omega - \frac{1}{2} \theta_1 \theta_2 R_l A_0^3 \Omega - \frac{1}{8} \theta_2^2 R_l A_0^5 \Omega - F_2\right) \sin(\tau) + \left(-\frac{1}{4} C_2 A_0^3 \Omega^2 - \frac{1}{4} C_3 A_0^3 \Omega^2 + \frac{1}{4} C_5 A_0^3\right) \cos(3\tau) + \left(-\frac{1}{2} \theta_1 \theta_2 R_l A_0^3 \Omega - \frac{3}{16} \theta_2^2 R_l A_0^5\right) \sin(3\tau) - \left(\frac{1}{16} \theta_2^2 R_l A_0^5 \Omega\right) \sin(5\tau) \tag{34}$$

Enforcing the coefficients of $\sin(\tau)$ and $\cos(\tau)$ to be equal to zero in order to avoid secular terms in the solution expression, and using the conditions in Eq. (11), we obtain the steady state solutions of the amplitude A_0 and the phase φ, respectively, as

$$\left[\left(-C_1 A_0 \Omega^2 - \frac{3}{4} C_2 A_0^3 \Omega^2 + \frac{1}{4} C_3 A_0^3 \Omega^2 + C_4 A_0 + \frac{3}{4} C_5 A_0^3\right)^2 + \left(-\theta_1^2 R_l A_0 \Omega - \frac{1}{2} \theta_1 \theta_2 R_l A_0^3 \Omega - \frac{1}{8} \theta_2^2 R_l A_0^5 \Omega\right)^2\right]^{\frac{1}{2}} = C_6 z_0 \Omega^2 \tag{35}$$

$$\varphi = \tan^{-1}\left(\frac{-\theta_1^2 R_l A_0 \Omega - \frac{1}{2} \theta_1 \theta_2 R_l A_0^3 \Omega - \frac{1}{8} \theta_2^2 R_l A_0^5 \Omega}{-C_1 A_0 \Omega^2 - \frac{3}{4} C_2 A_0^3 \Omega^2 + \frac{1}{4} C_3 A_0^3 \Omega^2 + C_4 A_0 + \frac{3}{4} C_5 A_0^3}\right) \tag{36}$$

Finally, solving the first-order deformation equation and using Eqs. (24) and (25), the first-order homotopy approximation of $v(t)$ becomes

$$v(t) = A u(\tau) \approx A_0(u_0(\tau) + u_1(\tau)) = \frac{c_0}{\Omega^2}\left[\left(\frac{\Omega^2}{c_0} A_0 - \frac{1}{32} C_2 A_0^3 \Omega^2 - \frac{1}{32} C_3 A_0^3 \Omega^2 + \frac{1}{32} C_5 A_0^3\right) \cos(\Omega t) + \left(-\frac{3}{16} \theta_1 \theta_2 R_l A_0^3 \Omega - \frac{9}{128} \theta_2^2 R_l A_0^5 - \frac{5}{384} \theta_2^2 R_l A_0^5 \Omega\right) \sin(\Omega t) + \frac{1}{32} (C_2 A_0^3 \Omega^2 + C_3 A_0^3 \Omega^2 - C_5 A_0^3) \cos(3\Omega t) + \left(-\frac{1}{16} \theta_1 \theta_2 R_l A_0^3 \Omega - \frac{3}{128} \theta_2^2 R_l A_0^5\right) \sin(3\Omega t) + \left(\frac{1}{384} \theta_2^2 R_l A_0^5 \Omega\right) \sin(5\Omega t)\right] \tag{37}$$

To obtain the solution for the voltage V, insert Eq. (37) into Eq. (6) considering the steady-state solution for large values of $t$as specified.

4 Discussion of results

The parameters for the beam, the tip mass and the energy harvester are given in Table 1. The model parameters were obtained from [4]. Due to the use of a double potential well, the post-buckled response has two equilibrium positions. The variation of the tip mass allows for three cases corresponding to pre-buckled, buckled and post-buckled responses. For our analysis we have chosen a value of 10.5g for the tip mass which lies in the post-buckling region.

Table 1. Parameter values for the beam and energy harvester

Beam and tip mass		Energy harvester	
ρ	7850 kg/m³	L_c	0.028 m
E	210 GN/m²	b_c	0.014 m
b	0.016 m	h_c	0.0003 m
h	0.000254 m	γ_c	-4× 10^{-5}Nm/V
$L = L_t$	0.3 m	C_p	51.4 nF
$\frac{I_t}{M_t}$	0.00004087 m²	R_l	10^5 Ω
Model parameters			
θ_1	-9.7703× 10^{-6}	N_8	1.0592× 10^4
θ_2	-2.9146× 10^{-7}	N_9	0.3669
N_1	0.0680	C_1	2.5738
N_2	0.1090	C_2	34.8460
N_3	0.9201	C_3	34.8460
N_4	4.1123	C_4	2.4244× 10^6
N_5	5.2360	C_5	3.3233× 10^7
N_6	112.7420	C_6	4.1182
N_7	772.7215	z_0	0.016

Figure 2 and 3 show the nonlinear time response and voltage output of the energy harvester for $t = 1400$ to $t = 1460$, respectively. They demonstrate that the output is considerably higher when the tip mass moves between the two equilibrium positions rather than when it is close to one of them. A value of $c_0 = 1$ was chosen.

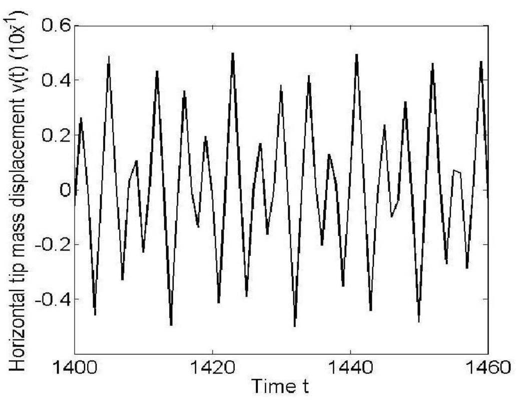

Fig. 2. Nonlinear time response of the energy harvester

In Fig. 4 the normalized amplitude-frequency curve is presented demonstrating the classical jump phenomenon for hardening-type nonlinearity. With respect to results obtained in [4], the outcomes are in close agreement the main difference being that an experimental result does not exhibit two coexisting solutions simultaneously and therefore jump phenomena in the amplitude-frequency curve may only be hinted at.

For the problem at hand, the standard simultaneous application of HAM for two coupled differential equations does not achieve unique solutions for the amplitude A and phase φ of the horizontal displacement $v(t)$ since the number of zero terms required to avoid secular terms in the final solution is greater than the number of unknown parameters. By this approach the amplitude of the horizontal displacement is derived to be a function of the external excitation frequency Ω and at the same time a fixed value independent from the harmonic base excitation.

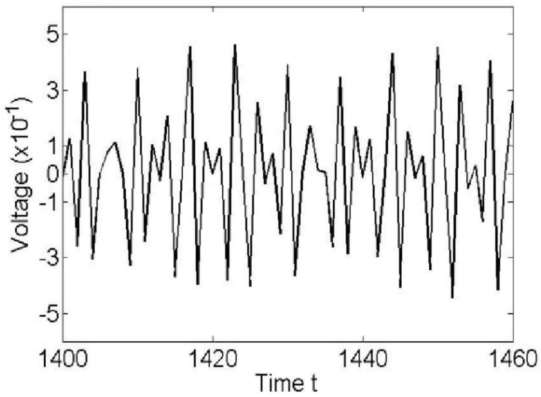

Fig. 3. Voltage output of the energy harvester

Moreover, zero initial conditions for the displacement and velocity of the tip mass used for the numerical analysis in [4] are not feasible when applying HAM, thus at $t = 0$, the vertical beam is displaced by an amplitude A to be determined. This is compatible with the beam's natural behavior.

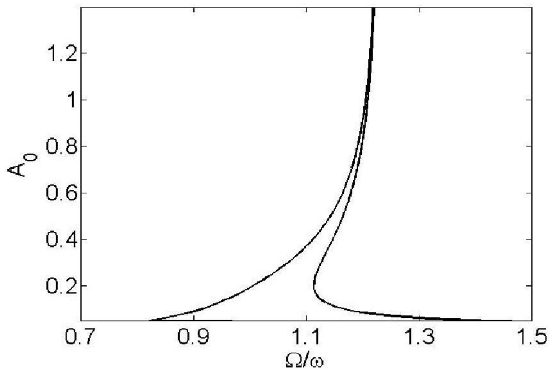

Fig. 4. Amplitude-frequency curve for values in Table 1

References

[1] A. Erturk, J. Hoffmann, D.J. Inman, Appl. Phys. Letters, **94**, 25, 1-3 (2009)

[2] A. Rysak, M. Müller, m. Borowiec, J. zubrzycki, G. Litak, Defence Sci Tech Agency, 508-512, (2013)

[3] I. Gammaitoni, I. Neri, H. Vocca, Appl. Phys. Lett. **94**, 16, 1-3 (2009).

[4] M.I. Friswell, S.F. Ali, O. Bilgen, S. Adhikari, A.W. Lees, G. Litak, J. Intel. Mat. Sys. Struct. **23**, 13, 1505-1521 (2012)

[5] S. Liao, *Beyond perturbation: Introduction to the homotopy analysis method* (CRC Press/Chapman Hall, Boca Rotan, 2003)

[6] S. Shahlaei-Far, A. Nabarrete, J.M. Balthazar, J. Theor. Appl. Mech. (to be published)